

# Analysis of location, acceleration, force and ductility parameters in buckling-restrained braced frames

Reza Jahanbakhshi

M.Sc. Department of Civil Engineering,  
Faculty of Engineering, Persian Gulf University

**Abstract - Sudden buckling and failure of bracing members in severe earthquakes reduces the efficiency of braced steel frames. The weakness can be modified and the efficiency of the bracing members can be increased by preventing the sudden buckling and failure of the bracing members.**

**In this dissertation, we introduce a new type of braces called buckling restrained braces (BRB). This brace consists of a steel core and a part resisting against buckling. Different models have been proposed for the buckling restrained part. But the most prevalent of which is the use of a concrete layer around the steel core. Understanding the components of this type of brace, we calculate the critical load of some samples of these braces using ANSYS software with the load obtained from the analysis being compared with the load calculated by the Euler relation.**

**Then, the behavior of ordinary buckling- restrained braced frames is compared in both linear and non-linear ways using El Centro seismic acceleration mapping. Bracing the frames is performed in two coaxial and eccentric ways. In the coaxial mode, 8-foot and braces are used, while in the eccentric mode, 8-foot open braces are applied.**

**To demonstrate the accuracy of the software, the results were compared with the those obtained by other researchers.**

**The results indicated that these types of braces serve as a damper in the frames by preventing the buckling of the member and were found to be very effective in reducing the structures being displaced in severe earthquakes.**

**Keywords:** buckling, braced frame, BRB

## Introduction

Lateral displacement of building structures has been the biggest concern of engineers. Designing for lateral displacement and lateral stability is an issue to be considered in the early stages of designing. Braced and flexural frames are systems widely commonly used in earthquake-prone areas. The frames in which lateral movement is controlled by applying brace members are called braced frames. A flexural frame, compared to a braced frame, appears with more lateral stiffness for the lateral displacement to be controlled. Using braced frames in buildings with steel frames provides an effective system for withstanding lateral loads. Therefore, extensive research has been done in recent years on braced frames, how these frames behave during earthquakes as well as the use of new braces.

One of the structural elements used as energy dissipators in metal frames is buckling- restrained bracing. This system is a type of lateral coaxial braces and usually runs in the form of 8. These elements are characterized by a very good energy dissipator. Buckling- restrained braces are called BRB. The frames braced with these elements (BRBFs) differ from conventional braced systems. This means that in conventional systems, the braces only withstand against tensions and pressure, while in frames with buckling restrained braces, the braces are also resistant to buckling. Research on buckling- restrained braces was first performed by Yoshino et al. In 1971 [1]. They tested two samples, they would call braced shear walls, made of a flat steel sheet covered by a concrete panel. Between the steel sheet and the concrete panel laid some non-sticking material. Yosami and Kaneko [3.2] conducted experiments on such sections in 2001.

One of the problems relates to the area where the brace is connected to the steel frame. In this type of brace, like conventional braces, metal plates (elastic) are used for the brace to be connected the steel frame. For this, the use of double cores is more common. The connection plate is laid between the two parts, welded or connected by bolts. These cores are either made completely in a double form or made double only at both ends (connection points).

Researchers have used other methods to avoid the core to have direct contact with the concrete cover. These methods include covering the steel core by silicone paint [4.5], VM tape or styrofoam [6.7.8-10], using two layers of polyethylene sheet with thickness of 0.15 and 0.20 mm [11.12], plastic sheets with thickness of 1.5 mm [13], thick silicone plastic sheet in 2 mm thickness [14], etc.

If these materials are not used, a gap or distance is made between the core and the coating mortar to create the necessary space for the relative deformation between the two members. The size of the gap varies depending on the type of BRB. The gap should be large enough to allow the core to expand. Otherwise, the friction created forces the buckling- restrained system to withstand part of the open axial load due to the interaction between the core and the concrete.

Researchers have tested various methods to analyze and design buckling- restrained braced frames. Energy and time history methods are used more than other methods.

According to the researches done by various researchers on this type of bracing and braced frames with it, it is seen that no comparison has been made between linear and non-linear analyses. That is, despite the fact that some researchers have studied the nonlinear behavior of such frames, they have not made a comparison with the linear analysis mode. This is while, most researches have only studied the behavior of coaxial braced frames (as 8 or diagonal) and the issue of eccentric braced frames has not been discussed.

In this study, in addition to a nonlinear analysis of buckling restrained braced frames, linear analysis was performed and the results were compared with the those obtained from linear and nonlinear analysis of conventional braced frames. In addition to coaxial braced frames, an eccentric braced frame was also examined.

### Materials and methods

#### Investigating the behavior of several types of buckling restrained braces

To determine the effect of coating concrete in preventing bracing buckling, the steel core of each model is once considered and its buckling load is obtained using Euler formula and software. Then, this process is repeated again for the core with concrete coating. In the end, the results are compared. The dimensions of the sections examined are given in Table (1).

Table (1): Dimensions of the sections examined (mm)

	Tube	Core
Cross-like	300*300*6	2 PL 250*28
Rectangular	300*300*6	PL 250*36
Circular	r = 42	r = 15

Some features of the samples are the same in all models and remain unchanged, i.e.,

- The length of the core, assumed to be 5 meters in all three models;
- The thickness of non-sticking material considered to be 2 mm in all models;
- Elastic modulus and Poisson ratio of steel, concrete and non-sticking materials used were the same in all models:

Investigating the steel core of models

The steel core is considered as a single-headed column, and we obtain the critical load. We use two methods to calculate the critical load:

- 1- Calculating the critical load using Euler formula

The critical load of a single-headed column is calculated according to the Euler relation as follows:

$$P_{cr} = \frac{\pi^2 EI}{4L^2} \quad (1)$$

Where  $P_{cr}$  is the critical load is in terms of Newton, E is the elasticity modulus by Pascal, I is the moment of inertia by cubic meters and L is the length in terms of meters.

#### Calculating the critical load using software

To calculate the critical load by the software, each sample should be first modeled by the specifications given in the software environment. To do this, the type of element used is first selected. A 3D element BEAM 188 has been used here. The model is divided into small elements after being meshed. Due to the fact that the surface section of the models varies, the number of elements created in each model is not the same. Now the type of analysis is selected and the Current LS section is chosen from the Solve menu so that the software can analyze the model.

Figures 1 show the models after meshing.

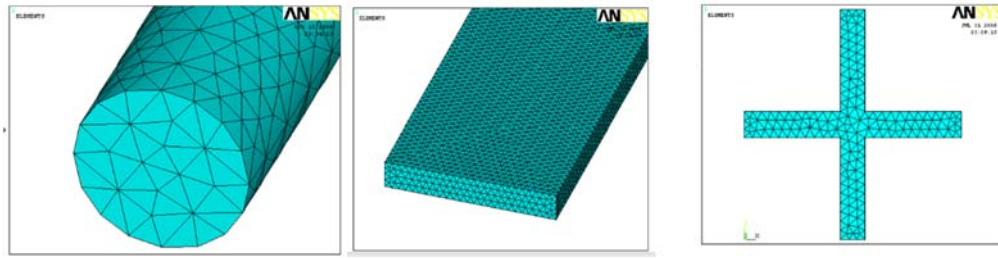


Figure 1: Meshing the models

The critical load created is compared in all three models as obtained by the two methods. The results are shown in Table (2).

Table (2) Comparison of critical load obtained in cores

Critical load Shape	(KN) $p_{cr}$		Disc. %
	Euler	ANSYS	
Cross-like	73.825	73.899	0.1
Rectangular	1.919	1.924	0.24
Circular	0.0786	0.0787	0.18

In the last column of Table 2, the discrepancy percentage for the critical load obtained through the software and the critical load obtained from the Euler formula is shown. By looking at these results, the accuracy of the results obtained from ANSYS software can be confirmed.

**Determining the target ductility ratio:**

The final displacement of the BRB is calculated based on the yield stress and the length of the brace as follows:

$$u_{by} = \frac{1}{\cos \theta} \frac{L_b}{E_b} \sigma_{by} \quad (2)$$

Where  $\theta$  is the angle that the BRB makes with the horizon surface;  $L_b$  is the length of BRB and  $E_b$  elasticity modulus of BRB.

Target displacement ( $u_T$ ) is specified. The ductility ratio of the target is equal to:

$$\mu_t = \frac{u_T}{u_{by}} \quad (3)$$

**Determining the required section for BRB:**

Determining the necessary section required for the BRB for the displacement intended is obtained by equating the hysterical energy and the energy scattered by the BRB:

$$E_h \times \sum_{i=1}^N m_i = \sum_{j=1}^N F_{yj} u_{yj} (\mu_a - 1) = (\mu_a - 1) \times \sum_{j=1}^N A_{bj} \sigma_{by} \frac{L_{bj} \sigma_{by}}{E_b} \quad (4)$$

Where  $E_h$  is the hysterical energy obtained from the spectrum;  $m_i$  is the  $i^{th}$  category mass;  $F_{yj}$  is the yield force of the  $j$  category,  $u_{yj}$  the final displacement of the  $j^{th}$  category;  $\mu_a$  ratio of total ductility and N is the number of categories.  $A_{bj}$ ,  $\sigma_{by}$ ,  $\theta_j$ ,  $L_{bj}$ , are the surface of section, length, angle and yield stress of the BRB positioned on the  $j^{th}$  category.

The BRB section surface on the  $j^{th}$  category is obtained by multiplying the section surface of the BRB positioned on the first category in the ratio of energy distribution in the -  $DR_j$  - categories.

$$A_{bj} = DR_j A_{b1} \quad (5)$$

From Equations (4) and (5) is obtained the surface section of the BRB of the first category:

$$A_{b1} = \frac{E_h \sum_{i=1}^N m_i}{(\mu_a - 1) \sum_{j=1}^N DR_j \sigma_{by} \frac{L_{bj} \sigma_{by}}{E_b}} \quad (6)$$

After calculating the BRB section of the first category, the BRB section of the other categories can be obtained from Equation (5).

**Investigating buckling- restrained brace**

To model the sample in the software, first the type of elements and specifications of consumables are introduced in the order mentioned in the previous section. The central part of the sample is then modeled. Then a layer of 2 mm thick is considered around the parts of the core placed inside the concrete. The steel tube is then placed around the core at a specified distance. Then between the tube and the core is filled with concrete. Of course, only the layers are made at this stage. Materials are attributed to these layers when meshing each layer is done.

Finally, after selecting the type of analysis, the software does the model analysis. The results obtained from the analysis of the models are given in Table (3).

Table (3) Results of model analysis

	No. of elements	No. of nodes	$P_{cr}$ (KN)
<b>Cross-like</b>	3440	404317	482.243
<b>Rectangular</b>	1958	125099	11.284
<b>Circular</b>	2369	175434	0.442

Figure (3) shows the displacement component in the y direction

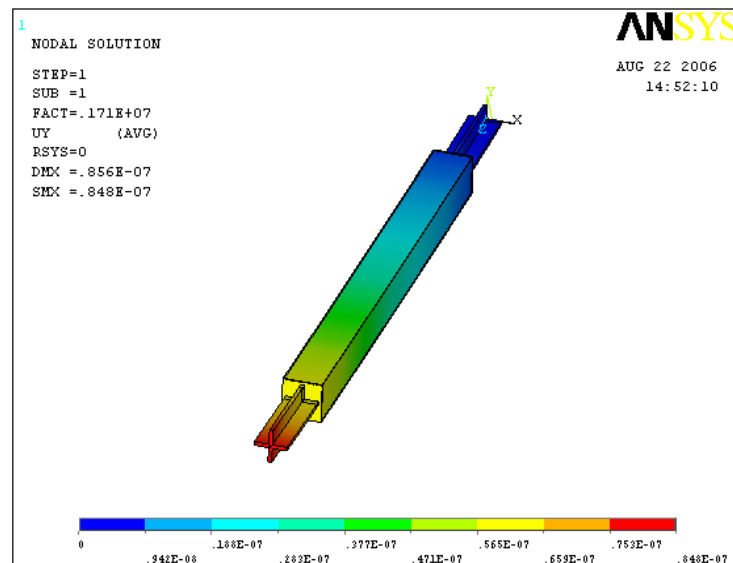


Figure (3) The displacement component in the y direction

Table (4) compares the buckling force generated in the BRB brace and the conventional brace. These forces are obtained by software.

Table (4) Comparison of buckling force obtained from software for BRB and conventional bracing

	$p_{cr}$ (KN)		$\frac{P_{cr(BRB)}}{P_{cr(core)}}$
	Conventional brace	BRB	
<b>Cross-like</b>	73.899	482.243	6.526
<b>Rectangular</b>	1.924	11.284	5.865
<b>Circular</b>	0.0787	0.442	5.616

As seen, the buckling load in the BRB brace increases significantly, and in the cross-like core model, this load increase is more than the other two models compared to the conventional brace.

**Investigating the accuracy of modeling done with ANSYS**

To demonstrate the accuracy of the modeling, the results are compared with the results obtained by other researchers. To determine the accuracy of the modeling performed by ANSYS software, the frame with a diagonal brace along with the specifications stated in Cheng Cheng Chen research (2001) is first modeled in the software environment and is placed under the L Centro earthquake record as well as nonlinear dynamic analysis. The results of this analysis were compared with the results expressed in the Chen study (2001).

Table (5) Comparison of the maximum displacement of categories in the braced frame with BRB bracing as a result of experiments on seismic table and analysis by ANSYS software

		Displacement (mm)					
		Seismic table			ANSYS		
Category	Type of frame	First	Second	Third	First	Second	Third
<b>Frame with a metallic brace</b>		11.2	21.1	32.3	10.6	21.8	32.4

The unimportant difference in the results of the two methods can be due to the following factors:

1-The sections used in the experimented frame on the seismic table were of a welded type. This is while in the model analyzed by the software, rolled sections have been used with the same dimensions.

2-In developing an experimental frame, it is possible to create discrepancies in the stiffness of the beam-to-column connections (due to human error in welding between parts, non-convergence of members in the nodes, etc.), while there are no such errors in the software.

3- Recording the results of practical experiments is not as accurate as computer analysis

**Analysis of buckling- restrained braced frames using ETABS software**

In the first step, the required sections for the braces must be determined. To do this, the models should be analyzed and designed with the dimensions and specifications given in the ETABS software under a specified load so that the required sections are obtained. The section intended for steel braces is angular (L-shaped sections). The specifications of this section are based on the specification table of building- Stahl profiles. For braces to resist buckling, a section with a square tube and a rectangular core is used. In order to select the appropriate section for the braces by the software, a list of these sections of different dimensions and sizes is placed in the section introduction part in ETABS software so that design is based on the appropriate section using the software's ability to automatically select the section.

After all sections were determined, each model was once entered in the ETABS software for a linearly dynamic analysis and in the ANSYS software for a nonlinear dynamic analysis.

Frame made of steel braces: The braces designed in this part are conventional steel made braces. In other words, in this part, the braced metal frame is examined. The sections obtained from a model analysis in ETABS software for steel braces are given in Table (6).

Table 6: Sections obtained for the steel braces from a model analysis in the ETABS software

Section Type of frame	Brace section		
	Floor	First	Second
Frame with a metallic brace	45*45*6L	40*40*6L	35*35*5L
Frame with 8 brace	40*40*4L	30*30*4L	25*25*3L
Frame with eccentric brace	40*40*6L	35*35*5L	30*30*4L

When the section of all braces was determined, the displacement related to the categories of each frame were plotted from the software outputs and the graphs were drawn.

The form changes diagram related to each of the frame categories obtained from a linear analysis of the frames in the ETABS software are presented in figures a to c.

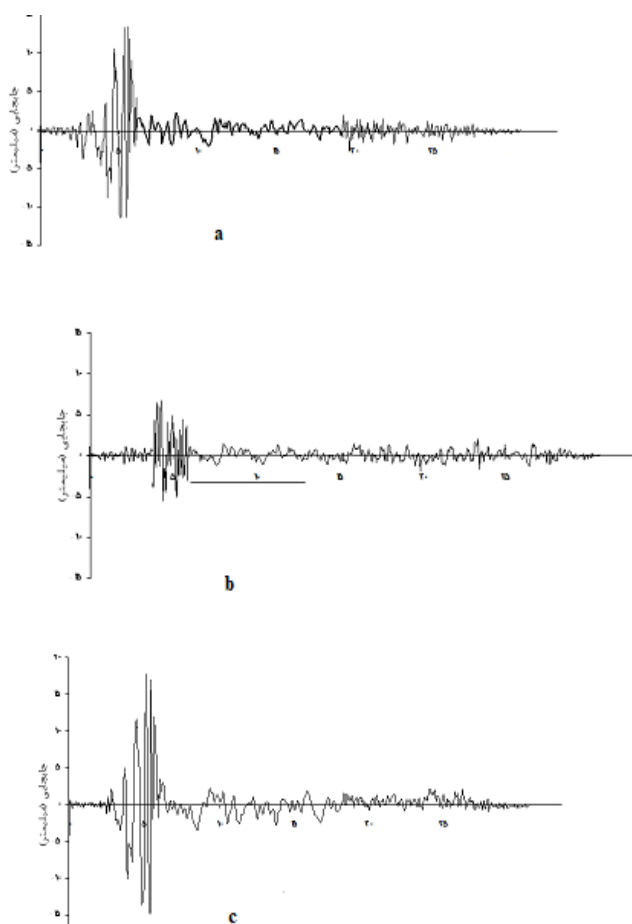


Figure 4- a) Changes in the form of the second category; the diagonal BRB braced frame from a linear analysis, b) Changes in the shape of the first category of the braced with BRB 8 from a linear analysis, c) Changes in the shape of the second category of the eccentric BRB brace from a linear analysis

Frame with BRB brace: In this part, the steel frame with buckling restrained brace is investigated. The section obtained for the core in the frame with the diagonal bracing is almost the same with the section used in the model tested on the seismic table. For example, the core dimensions on the ground floor of the model built are 26 x10 mm on the seismic table, and in the model built in ANSYS software, it is 25 x 10 mm.

The diagram of shape change related to the categories of each frame obtained from a nonlinear frame analysis in the ANSYS software is shown in Figures 5a to c.

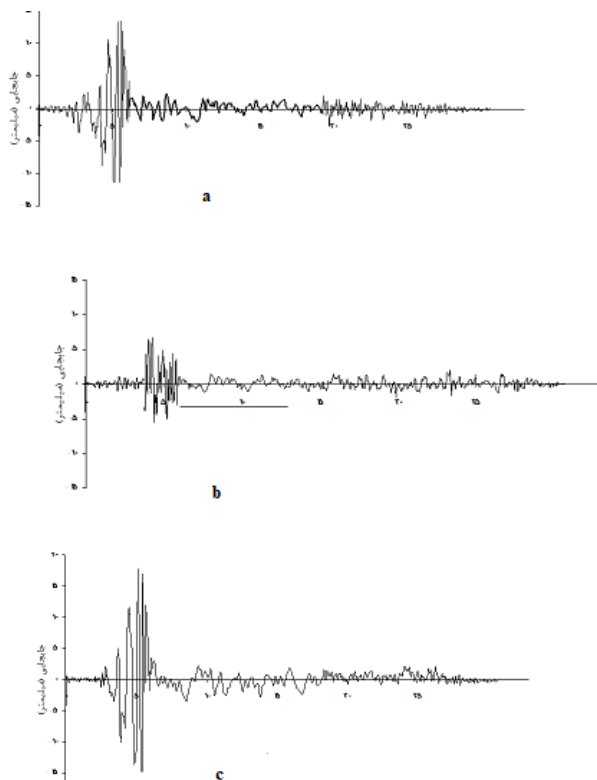


Figure 5- a) Changes in the form of the second category; the diagonal BRB braced frame from a linear analysis, b) Changes in the shape of the first category of the braced with BRB 8 from a linear analysis, c) Changes in the shape of the second category of the eccentric BRB brace from a linear analysis

The acceleration diagram of the different levels for each frame obtained from a nonlinear analysis of the frames in ANSYS software are shown in Figures 6a to c.

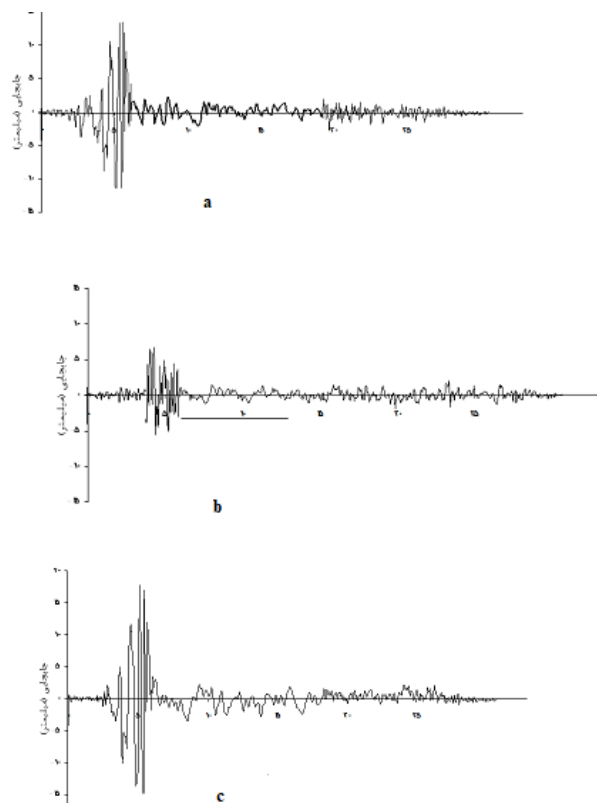


Figure 6- a) Changes in the form of the second category; the diagonal BRB braced frame from a linear analysis, b) Changes in the shape of the first category of the braced with BRB 8 from a linear analysis, c) Changes in the shape of the second category of the eccentric BRB brace from a linear analysis

In Figures 7a to c, the modeled frames are shown after being analyzed by the software.

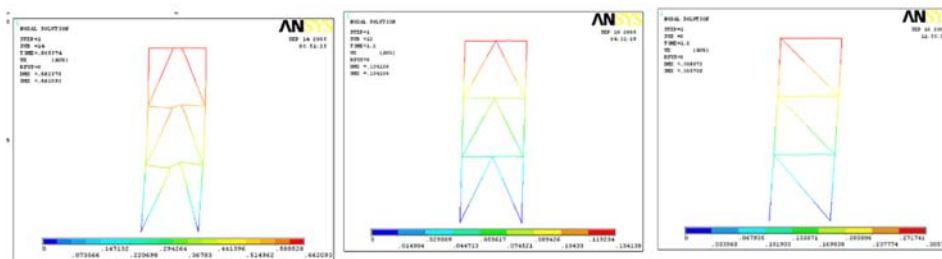


Figure 7 Diagonal braced frames, b) Braced frame 8, c) Eccentric braced frame

### Results

#### Maximum displacement

The maximum displacement of the frames from a linear and non-linear analysis under the El Centro earthquake record is provided in Table (7). These values relate to the displacement in the roof level of each frame.

Table (7) Comparison of maximum displacement created in braced frames with steel brace and BRB from a linear and nonlinear analysis

Category Type of frame		Displacement (mm)			
		Linear analysis		Non-linear analysis	
		Conventional brace	BRB	Conventional brace	BRB
Frame with diagonal brace		22.8	19.3	47.0	32.4
Frame with brace 8		19.1	12.1	32.6	20.3
Frame with eccentric brace		26.2	25.7	73.5	58.4

As seen in Table (7), the displacement of frames from a nonlinear analysis is higher than that in the linear analysis, which is quite logical.

#### Ductility coefficient

Ductility coefficient is the ratio of the maximum final deformation of the structure to the deformation at the yield moment. The maximum displacement of categories in frames braced with conventional bracing and BRB bracing from nonlinear analysis under the El Centro earthquake record is provided in Table (8).

Table (8) Form change of moment of yield in the floors in braced frames with steel bracing and BRB from a nonlinear analysis

Category Type of frame		Form change of yield moment (mm)					
		Conventional frame			BRB		
		First	Second	third	First	Second	third
Frame with diagonal brace		4.1	7.3	8.0	5.2	7.8	9.0
Frame with brace 8		4.6	5.2	8.1	4.2	8.5	10.6
Frame with eccentric brace		7.8	9.3	12.5	6.1	11.3	14.4

As seen from the results in Table (8), braced frames with conventional brace yield sooner and with less displacement.

Using the ductility coefficient relation, the ductility of the categories is obtained from a nonlinear analysis as the values provided in Table 9.



Table (9) Class ductility coefficient from a nonlinear analysis

Category Type of frame		Ductility					
		Conventional brace			BRB		
		First	Second	Third	First	Second	Third
Frame with diagonal brace		7.6	5.5	5.9	2.0	2.8	3.6
Frame with brace 8		4.3	5.4	4.0	2.0	1.3	1.9
Frame with eccentric brace		6.6	7.3	5.9	5.5	3.7	4.1

According to Table (9), the following results are obtained:

- 1- Using BRB as a brace in steel frames reduces the ductility coefficient.
- 2- The stiffer the frame, the lower its ductility.

**Maximum category acceleration**

The maximum acceleration of the categories is as follows:

Table (10) Comparison of maximum acceleration created in braced frames with steel bracing and BRB from a linear and nonlinear analysis

Category Type of Frame		Acceleration (m/s)			
		Linear analysis		Non-linear analysis	
		Conventional brace	BRB	Conventional brace	BRB
Frame with diagonal brace		4.54	5.21	3.94	4.88
Frame with brace 8		4.85	5.39	4.18	5.02
Frame with eccentric brace		4.12	5.14	3.85	4.51

According to the results in Table 10, the findings are as follows:

- 1- The acceleration created in the categories from a linear analysis is higher than the corresponding acceleration obtained from a nonlinear analysis.
- 2- The acceleration of the categories in the braced frames with buckling restrained braces is higher than the frames braced with conventional braces.
- 3- The harder the frame, the greater the acceleration in it. As a result, the acceleration generated in the frame with brace 8 is higher than the frame with diagonal brace and it is greater than the frame with eccentric brace.
- 4- The acceleration of the lower categories is less than that of the upper categories.

**The force created in the category brace**

After the models were analyzed in both linear and nonlinear modes, the internal force of each brace member was obtained from the software outputs and provided in Table 11.

Table (11) The force created in the braced frames with steel bracing and BRB from a linear and nonlinear analysis

Category Type of frame		Force (kN)					
		Conventional brace			BRB		
		Ground floor	First	Second	Ground floor	First	Second
Frame with diagonal brace		50.9	32.9	16.3	64.9	40.5	18.7
Frame with brace 8		42.2	25.9	13.2	53.1	31.5	14.6
Frame with eccentric brace		44.0	26.8	12.8	56.9	33.7	16.0

Non-linear		Force (kN)					
		Conventional brace			BRB		
Category	Type of frame	Ground floor	First	Second	Ground floor	First	Second
	Frame with diagonal brace	42.7	28.8	13.9	59.5	37.3	17.6
	Frame with brace 8	38.5	23.4	11.4	48.9	29.2	13.6
	Frame with eccentric brace	39.2	23.8	12.0	50.8	30.0	14.0

According to the results provided in Table 11, the following are obtained:

- 1- The force created in the category bracing from a linear analysis is greater than the corresponding force obtained from a nonlinear analysis.
- 2- The force created in the category bracing in braced frames with buckling restrained bracing is greater than the braced frames with conventional bracing.
- 3- The harder the frame, the more force will be generated in the category bracing. Because in a frame braced with a diagonal brace, only one member in each category is responsible for bearing the lateral load, the force created in this type of brace is greater than the other two types of braces.
- 4- The force generated in the lower category braces is greater than the upper categories.

### Conclusion

According to the results from comparing buckling restrained braced frames with conventional braced frames made from different directions, it is possible to understand this member as a damper in absorbing seismic energy of the structure and reducing lateral displacement. As seen from comparative diagrams of the behavior of braced frames with buckling restrained brace, using this member as 8 in coaxial braced frames will yield greater efficiency than diagonal and eccentric models. In other words, using BRB in form of 8 in bracing steel frames causes a higher percentage of seismic energy of the structure to be absorbed due to an earthquake, resulting in significant reduction of lateral displacement of the structure.

Obviously, reducing the lateral displacement of the structure will have a significant impact on the design of other structural members, i.e., beams and columns. This is because as the stiffness of the structure increases, the sections of the beams and columns will become weaker. Therefore, using this member as a brace in steel structures will lead to lighter structures and cost-saving in terms of steel consumption.

### References

- [1] Usami, T., Kaneko, H., Ono, T. (2002). □Strength of H-shaped brace constrained flexural buckling having unconstrained area at both ends: both ends fixed. □ Journal of Structural and Construction Engineering, pp. 211–218.
- [2] Suzuki, N., Kono, R., Higashibata, Y., Sasaki, T., Segawa, T. (1994). □Experimental study on the H-section steel brace encased in RC or steel tube. □ Summaries of technical papers of annual meeting, vol. II, Architectural Institute of Japan, C, Structural Engineering Section, pp. 1621–1622.
- [3] Inoue, K., Sawaiyumi, S., Higashibata, Y., Inoue, K. (1992). □Bracing design criteria of the reinforced concrete panel including unbonded steel diagonal braces. □ Journal of Structural and Construction Engineering, Architectural Institute of Japan, pp. 41–49.
- [4] Fujimoto, M., Wada, A., Saeki, E., Watanabe, A., Hitomi, Y. (1988). □A study on the unbonded brace encased in buckling-restraining concrete and steel tube. □ Journal of Structural and Construction Engineering, pp. 249–258.
- [5] Watanabe, A., Hitomi, Y., Saeki, E., Wada, A., Fujimoto, M. (1988). □Properties of brace encased in buckling-restraining concrete and steel tube. □ In: Proc. of ninth world conf. on earthquake eng., vol. IV, pp. 719–724.
- [6] Saeki, E., Maeda, Y., Nakamura, H., Midorikawa, M., Wada, A. (1995). □ Experimental study on practical-scale unbonded braces. □ Journal of Structural and Construction Engineering, pp. 149–158.
- [7] Saeki, E., Iwamatu, K., Wada, A. (1996). □Analytical study by finite element method and comparison with experiment results concerning buckling-restrained unbonded braces. □ Journal of Structural and Construction Engineering, pp. 111–120.
- [8] Saeki, E., Maeda, Y., Iwamatu, K., Wada, A. (1996). □Analytical study on unbonded braces fixed in a frame. □ Journal of Structural and Construction Engineering, pp. 95–104.
- [9] Tada, M., Kuwahara, S., Yoneyama, T., Imai, K. (1993). □Horizontally loading test of the steel frame braced with double-tube members. □ Annual technical papers of steel structures, vol. 1, pp. 203–208.
- [10] Manabe, N., Simokawa, H., Kamiya, M., Morino, S., Kawaguchi, J. (1996). □Elasto-plastic behavior of flat-bar brace stiffened by square steel tube. □ Summaries of technical papers of annual meeting, vol. III, pp. 783–784.
- [11] Murakami, E., Mitarai, Y., Asayama, N., Narihara, H. (1999). □Experiment on retrofitting of existing brace improved to unbonded brace. □ Summaries of technical papers of annual meeting, vol. III, Architectural Institute of Japan, Structural Engineering Section, pp. 843–844.
- [12] Tsai KC, Weng CH. Experimental responses of double-tube unbonded brace elements and connections. Report No. CEER/R91-02, Center for Earthquake Engineering Research, National Taiwan University; 2002